

Effect of Gas Permeation Temperature and Annealing Procedure on the Performance of Binary and Ternary Mixed Matrix Membranes of Polyethersulfone, SAPO-34, and 2-Hydroxy 5-methyl Aniline

Edibe Eda Oral, Levent Yilmaz, Halil Kalipcilar

Department of Chemical Engineering, Middle East Technical University, 06800 Ankara, Turkey

Correspondence to: H. Kalipcilar (E-mail: kalipcil@metu.edu.tr)

ABSTRACT: This study investigated the effect of annealing time and temperature on gas separation performance of mixed matrix membranes (MMMs) prepared from polyethersulfone (PES), silicoaluminophosphate (SAPO-34), and 2-hydroxy 5-methyl aniline (HMA). A postannealing period at 120°C for a week extensively increased the reproducibility and stability of MMMs, but for pure PES membranes no post-annealing was necessary for stable and reproducible performance. The effect of operation temperature was also investigated. The permeabilities of H₂, CO₂, and CH₄ increased with increasing permeation temperature from 35°C to 120°C, yet CO₂/CH₄ and H₂/CH₄ selectivities decreased. PES/SAPO-34/HMA ternary and PES/SAPO-34 binary MMMs exhibited the highest ideal selectivity and permeability values at all temperatures, respectively. For H₂/CO₂ pair, when temperature increased from 35°C to 120°C, selectivity increased from 3.2 to 4.6 and H₂ permeability increased from 8 to 26.5 Barrer for ternary MMM, demonstrating the advantage of using this membrane at high temperatures. The activation energies were in the order of CH₄ > H₂ > CO₂ for all membranes. PES/SAPO-34/HMA membrane had activation energies higher than that of PES/SAPO-34 membrane, suggesting that HMA acts as a compatibilizer between the two phases. © 2014 Wiley Periodicals, Inc. *J. Appl. Polym. Sci.* **2014**, *131*, 40679.

KEYWORDS: membranes; porous materials; separation techniques; thermal properties

Received 10 September 2013; accepted 4 March 2014

DOI: 10.1002/app.40679

INTRODUCTION

The performance of gas separation membranes is often determined at a temperature range of 25–35°C. The well-known Robeson upper bound curve was also developed based on the membrane performances at this temperature range.^{1–3} The effect of temperature on the upper bound curves has been developed recently.³ As the industrial applications take place in a much wider temperature range, the effect of temperature on separation performances of membranes should be known.

The permeabilities in polymeric membranes are related to polymer structure and also the polymer penetrant interactions, which are influenced by temperature strongly.³ It is generally observed that permeabilities increased but selectivities decreased with increasing permeation temperature. Higher permeabilities are usually attributed to increased flexibility of polymer chains with temperature, which even compensate the decrease of solubilities.^{4–6}

A similar effect of temperature was observed for mixed matrix membranes (MMMs). Jha and Way⁷ studied the silicoaluminophosphate (SAPO-34) filled rubbery poly dimethyl sulfoxide MMMs and investigated the effect of temperature between –15°C and 22°C.

The highest CO₂/CH₄ ideal selectivity, which was approximately 58, was obtained at –15°C. It decreased to approximately 18 when the permeation temperature was 22°C. Choi et al.⁸ studied the separation of H₂/CO₂ by polybenzimidazole (PBI), swollen amhert-3 (AMH-3), and proton-exchanged AMH-3 incorporated PBI composite membranes between 35°C and 200°C. At 35°C the ideal selectivities of composite membranes were approximately 40, which were nearly four times higher than that of pure PBI membranes. At 200°C H₂ and CO₂ permeabilities increased but the ideal selectivities of composite membranes decreased and approached to the ideal selectivities of pure PBI membranes.

MMMs prepared from glassy polymers and inorganic particles have usually suffered from voids formed at the polymer–particle interface, which significantly reduced the membrane performance. Many methods have been carried out to eliminate these voids by modifying the membrane materials. One approach is incorporation of additives with functional groups as the third component into the membrane.^{9–11} Those additives were silane coupling agents like 3-aminopropyltriethoxysilane to modify the zeolite surface or low-molecular-weight compounds like *p*-nitroaniline and 2-hydroxy 5-methyl aniline (HMA) to modify the polymer. The effect of temperature on the gas permeation

through ternary component membranes was barely investigated. Khan et al.¹² studied the gas permeation performance of acrylate-modified polysulfone/zeolite 3A/aminopropyltrimethoxysilane at different temperatures. They observed that H₂ permeability increased whereas the H₂/CO₂ selectivity decreased with increasing temperature.

Our group has studied the gas permeation and separation characteristics of ternary component MMMs prepared by using low-molecular-weight compounds at a permeation temperature of 25°C–35°C.^{9,13,14} This kind of membranes has not been tested at elevated temperatures. The objective of the present study was, therefore, to investigate the effect of gas permeation temperature on the performance of polymer/zeolite/additive MMMs. The membranes used in this study were pure polyethersulfone (PES) membrane, PES/HMA (4% w/w) membrane, PES/SAPO-34 (20% w/w) MMM, and PES/SAPO-34 (20% w/w)/HMA (4% w/w) MMM. The membranes were tested by measuring the permeabilities of H₂, CO₂, and CH₄ between 35°C and 120°C.

For membranes prepared by solvent evaporation method, solvent type, evaporation conditions, and the amount of residual solvent in the membrane can influence the final properties and the gas separation performance of membranes.^{8,14} Hacırlıoğlu et al.¹⁵ observed that the removal of residual solvent yielded higher selectivities but lower permeabilities, which was attributed to the densification of membranes by the removal of residual solvent.¹⁶ Similarly Maeda and Paul^{17,18} observed increased selectivities but reduced permeabilities when low-molecular-weight solvents were incorporated into the membrane because of the antiplasticization effect of these compounds. Fu et al.¹⁹ showed that the role of the residual solvent, either plasticizer or antiplasticizer, depends on the amount of residual solvent in the membrane. Joly et al.²⁰ showed that, as the amount of residual solvent in the fluorinated polyimide membranes decreased, the diffusion coefficient decreased but permeabilities increased.

Annealing is the thermal treatment, which is applied to remove the remaining solvent in the membrane. Studies investigating the effect of annealing temperature and time on the membrane performance were generally conducted for pure polymeric membranes. The present study also reports the effect of annealing conditions on the performance of PES/SAPO-34 and PES/HMA/SAPO-34 MMMs.

Gas separation membranes are expected to exhibit high permeabilities and high selectivities for industrial applications like natural gas sweetening and separation of refinery gases. All industrial applications require membranes with stable performance upon exposure to high and low temperatures and pressures during its service life. In this study, membranes had been tested for more than 1 month at temperatures between 35°C and 120°C.

EXPERIMENTAL

Materials

Radel A-100 grade PES (Solvay) with a molecular weight of 53,000, dimethylformamide (DMF; Acros, $T_{b,p} = 153^\circ\text{C}$), and HMA (Acros, $M_w = 123.16$, $T_{m,p} = 137^\circ\text{C}$) were used in mem-

brane preparation. PES was dried overnight at 100°C to remove the adsorbed water before the membrane preparation.

SAPO-34 crystals were used as inorganic filler. Ludox AS-40 (Aldrich), tetraethylammonium hydroxide (TEAOH, 20 wt % in water, Acros), pseudoboehmite (98%, Acros), phosphoric acid (85 wt %, Acros), and deionized water were used to synthesize SAPO-34.

Synthesis of SAPO-34

SAPO-34 was crystallized from a synthesis gel with a molar composition 1 Al₂O₃ : 1 P₂O₅ : 0.4 SiO₂ : 2 TEAOH : 71.5 H₂O. Pseudoboehmite was dissolved in Ludox AS-40 and TEAOH mixture. Hydrothermal treatment was carried out by two-stage variable temperature method. Aging at 80°C for 24 h was followed by crystallization at 200°C for 24 h. The powder was recovered by centrifuging the resulting suspension and was washed with DI water for two times. Finally, it was dried overnight at 80°C. Calcination was carried out at 500°C for 3 h with a heating/cooling rate of 1.5°C/min in air to remove the organic template from the pores. Before membrane preparation, SAPO-34 crystals were treated at 250°C for 24 h to remove the physically adsorbed water.

Membrane Preparation

Four types of membranes, namely pure PES, PES/HMA, PES/SAPO-34 binary mixed matrix, and PES/SAPO-34/HMA ternary MMMs, were prepared by solvent-evaporation method from solutions with 20% (w/v) PES in DMF. The percentages of SAPO-34 and HMA in the membranes were 20% (by weight) and 4% (by weight), respectively.

To prepare a ternary MMM, SAPO-34 was dispersed in DMF, and the mixture was ultrasonicated for 60 min to minimize the agglomeration. Then, HMA was added, and the mixture was stirred overnight by a magnetic stirrer. 15% (w) of total amount of PES was introduced to the mixture and kept in ultrasonic bath for 60 min.²¹ Then, the remaining amount of the polymer was added gradually. After each addition of PES, the mixture was ultrasonicated. The final mixture was blade cast on a glass plate at room temperature in air using a film applicator, with a casting knife clearance of 500 μm. The membrane was obtained after evaporation at 80°C and 0.2 bar for 8 h and annealing at 100°C and 1 bar N₂ for 24 h. Some of the membranes were post-annealed at 120°C and 0.2 bar N₂ for 7–30 days.

Membrane Characterization

Thermal characterizations of the membranes were conducted using differential scanning calorimetry (Shimadzu DSC60) and thermal gravimetric analysis (TGA, Shimadzu DTG-60H). For TGA analysis, the samples were heated from 30°C to 250°C at a heating rate of 10°C/min with a N₂ flow rate of 75 mL/min. For differential scanning calorimetry analysis, the membrane samples were heated from 30°C to 250°C at a rate of 10°C/min in N₂ atmosphere for the first scan. The sample was then cooled to 30°C for the second scan at same conditions. The data from the second scan were used to determine the T_g . The morphological characterizations of the membranes coated with gold/palladium were performed using scanning electron microscopy (SEM, FEI Quanta-400 F).

Constant volume variable pressure technique was used for single gas permeation measurements of H₂, CO₂, and CH₄. Membrane

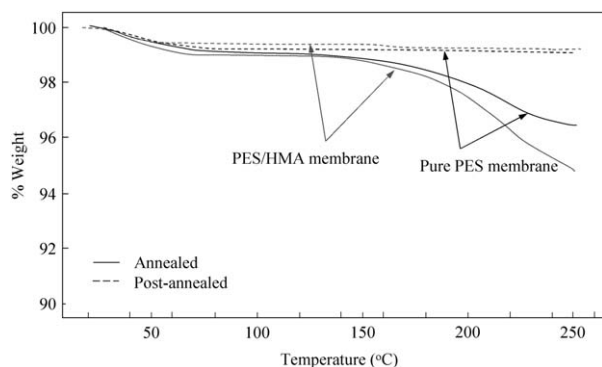


Figure 1. TGA curves of pure PES and PES/HMA membranes. The solid lines are for annealed membranes, and the dashed lines are for post-annealed membranes.

module was a commercial module Millipore filter holder (Millipore, part no.XX45 047 00) with double-Viton O-ring seal. The effective membrane area was 9.6 cm^2 , and the dead volume of the system was 7.1 cm^3 . Before each measurement, both feed and permeate sides were evacuated by a vacuum pump (Model E2M5, Edwards high vacuum pump) to less than 0.1 bar for at least 1 h. The high pressure feed (2.9 bar) permeated through the membrane, and the increase in the permeate side pressure was monitored to calculate the permeability. The pressure increase in the permeate side was monitored with a pressure transducer (BD Sensors, DMP331, 0–4 bar pressure range, 0.001 bar sensitivity). The ratio of single gas permeabilities is defined as the ideal selectivity.

The membrane module was placed in a silicone oil bath. The permeation temperature was changed between 35°C and 120°C . The gas permeation through a particular membrane was carried out first for H_2 , then for CO_2 , and finally for CH_4 at 35°C ; then the temperature was increased to a new set point, and the permeabilities of all gases were measured again in the same order. After all temperature changes, the system was cooled, and the permeation measurements were conducted at 35°C again.

RESULTS AND DISCUSSION

Thermal Analysis of Membranes

Figure 1 shows the TGA thermograms of PES-n and -p and PES/HMA-n and -p membranes (hereafter -n and -p represent the membranes annealed and post-annealed, respectively). All membranes lost approximately 1% of their weight below 100°C regardless of whether annealed or post-annealed. This weight loss can be attributed to the release of moisture sorbed and other minor contaminants by the membranes.^{22,23}

The PES-n and PES/HMA-n membranes exhibited relatively high weight loss above 150°C possibly due to the removal of residual solvent. On the other hand, the weight of PES-p and PES/HMA-p membranes remained constant above 150°C , showing the thermal stability of post-annealed membranes and indicating that post-annealing resulted in the removal of additional amount of solvent from the membranes. Figure 2 shows TGA thermograms of SAPO-34-containing MMMs, which exhibit very similar trend with the thermograms of the neat polymeric membranes. The weight loss was approximately 4% below

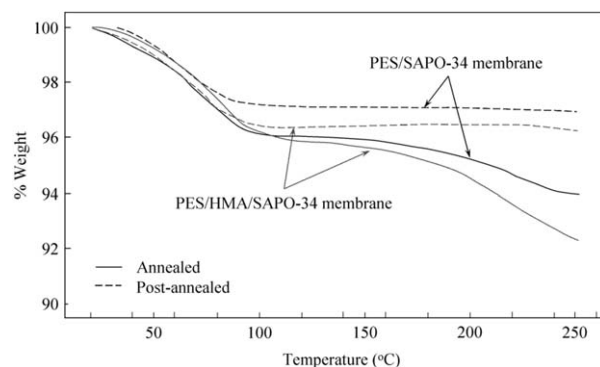


Figure 2. TGA curves of PES/SAPO-34 and PES/HMA/SAPO-34 membranes. The solid lines are for annealed membranes, and the dashed lines are for post-annealed membranes.

100°C for both types of membranes. The weight of post-annealed membranes remained almost constant above 150°C , whereas that of membranes, which were not post-annealed, decreased further at temperatures above 150°C .

The amount of residual solvent was higher in SAPO-34-containing membranes because zeolite crystals and the interfacial voids surrounding these crystals may seize solvent and moisture. The TGA results indicated that membranes that annealed regularly included some solvent and post-annealing promotes the removal of remaining solvent.

Effect of Residual Solvent on Gas Permeation

To investigate the effect of residual solvent for both dense homogenous membranes and MMMs, the permeabilities of all gases were measured by changing the measurement temperature between 35°C and 90°C cyclically (such as $35^\circ\text{C} \rightarrow 90^\circ\text{C} \rightarrow 35^\circ\text{C} \rightarrow 90^\circ\text{C}$ and so on). Total duration of measurements was longer than 1 month for each membrane. First, this routine was applied to the annealed pure PES-n and PES/SAPO-34-n membranes (annealed at 100°C , 0.2 bar, 8 h). Permeabilities of H_2 , CO_2 , and CH_4 through these two membranes are reported as a function of order of measurement in Figure 3 for PES-n and in Figure 4 for PES/SAPO-34-n membranes.

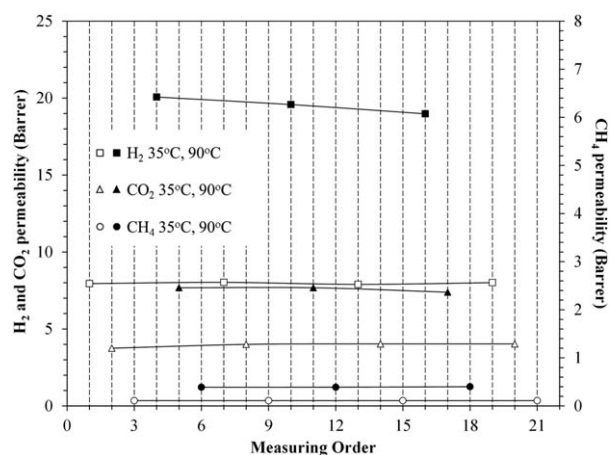


Figure 3. Single gas permeabilities of H_2 , CO_2 , and CH_4 through annealed pure PES membrane at 35°C and 90°C .

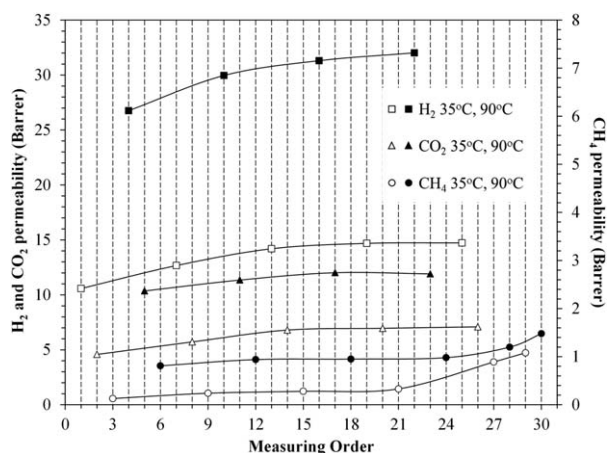


Figure 4. Single gas permeabilities of H₂, CO₂, and CH₄ through annealed PES/SAPO-34 membrane at 35°C and 90°C.

Pure PES membrane exhibits a stable performance for all gases; for instance CH₄ permeability was found as 0.1 Barrer in all measurements at 35°C and as 0.4 Barrer at 90°C. On the other hand, the permeabilities of all gases increased with repeating measurements for PES/SAPO-34 membrane; for instance H₂ permeability was first 26.8 Barrer and finally 32.0 Barrer at 90°C. Similarly, CH₄ permeability increased from 0.8 to 1.6 Barrer at 90°C after all. A similar trend was also observed at 35°C for all gases. Among all gases, the change was more noticeable for CH₄, so that the final CH₄ permeability was 8 and 1.8 times as high as the initial CH₄ permeability at 35°C and 90°C, respectively.

The same cyclical measurement routine was also applied for post-annealed MMMs. Figure 5 shows the H₂, CO₂, and CH₄ permeabilities of PES/SAPO-34 membrane after post-annealing at 120°C, in 0.2 atm N₂, for 7 days. The membrane exhibited a very stable performance so that the permeabilities for each gas remained constant throughout the measurements.

The residual solvent, which partly occupies the free volume of the polymer, influences the gas permeabilities through a membrane.²⁴ No change in the permeabilities was observed for PES-n

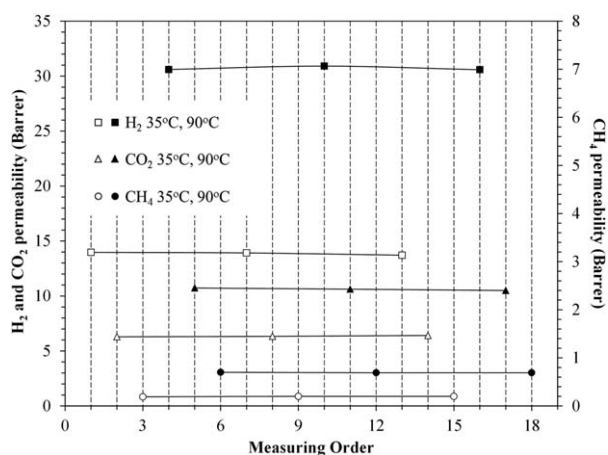


Figure 5. Single gas permeabilities of H₂, CO₂, and CH₄ through post-annealed PES/SAPO-34 membrane at 35°C and 90°C.

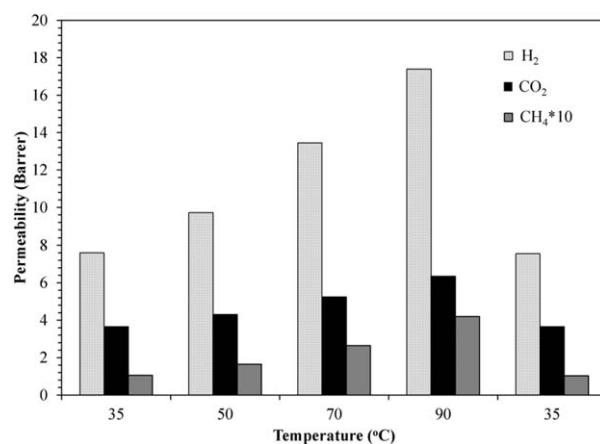


Figure 6. Change in single gas permeabilities with temperature for annealed PES membrane.

membrane after successive measurements between 35°C and 90°C, indicating that all solvent was successfully removed from this membrane during the annealing process. On the other hand, the solvent can be held by SAPO-34 particles in the PES/SAPO-34-n membrane; therefore, SAPO-34-containing membranes need longer annealing periods at higher temperatures. The membranes that had been post-annealed at 120°C, in 0.2 atm N₂ at least for 1 month, exhibited higher permeabilities and more stable membrane performances.

Effect of Operating Temperature on Membranes Performance

The effect of temperature on the performance of membranes was studied in the temperature range of 35°C–120°C. Pure PES membrane was used only after regular annealing because its performance did not show a substantial change after many repetitive measurements.

Figures 6–9 show the permeabilities of studied gases as a function of permeation temperature for PES-n, PES/HMA-p, PES/SAPO-34-p, and PES/HMA/SAPO-34-p membranes, respectively. Gas permeabilities increased with temperature for all membranes (Figures 6–9). The H₂ permeabilities through PES/HMA and PES/HMA-SAPO-34 membranes increased by nearly

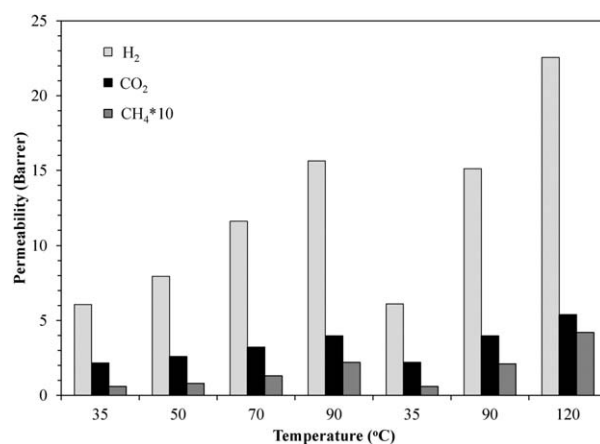


Figure 7. Change in single gas permeabilities with temperature for post-annealed PES/HMA membrane.

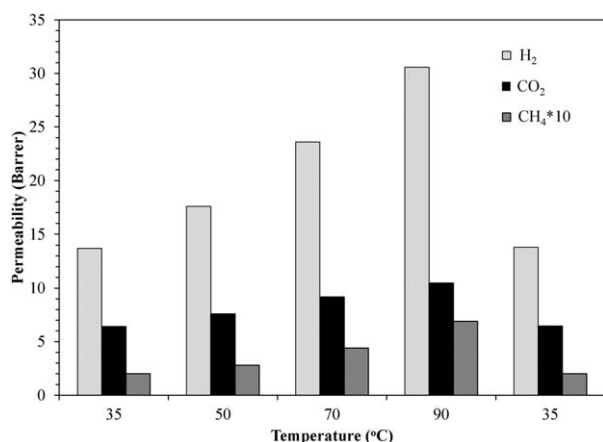


Figure 8. Change in single gas permeabilities with temperature for post-annealed PES/SAPO-34 membrane.

269% and 233%, respectively, when the permeation temperature was changed from 35°C to 120°C. A similar trend was also observed for CO₂ and CH₄. The solution-diffusion mechanism is often used to describe the gas permeation through polymeric membranes. This mechanism involves the sorption of gases by the membrane at the feed side, followed by diffusion through the membrane, and finally desorption from the permeate side. High temperatures facilitate the motion of polymer chains, which results in larger diffusion coefficients but lower solubilities for all gases.^{4,25} Substantially high permeabilities at 120°C indicate that the increase in diffusion coefficients compensates the decrease in solubilities.

HMA-incorporated membranes exhibited substantially lower permeabilities than the HMA-free counterparts at all temperatures in the studied range. For instance, PES-n and PES/HMA-p showed H₂ permeabilities of 18.6 and 15.1 Barrer at 90°C. Similarly, the H₂ permeability through PES/SAPO-34 membrane at 90°C was greater than that through PES/HMA/SAPO-34-p by 39%. HMA was shown to have antiplasticization effect on PES matrix at 35°C.^{13,14} Apparently, antiplasticization effect holds even at higher temperatures, indicating that HMA strongly interacts with PES during the membrane preparation and is a

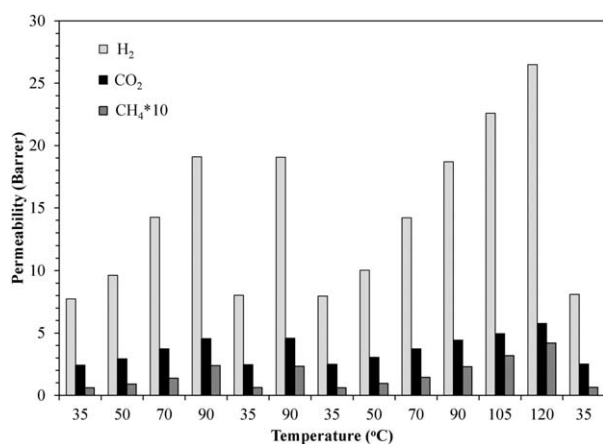


Figure 9. Change in single gas permeabilities with temperature for post-annealed PES/HMA/SAPO-34 membrane.

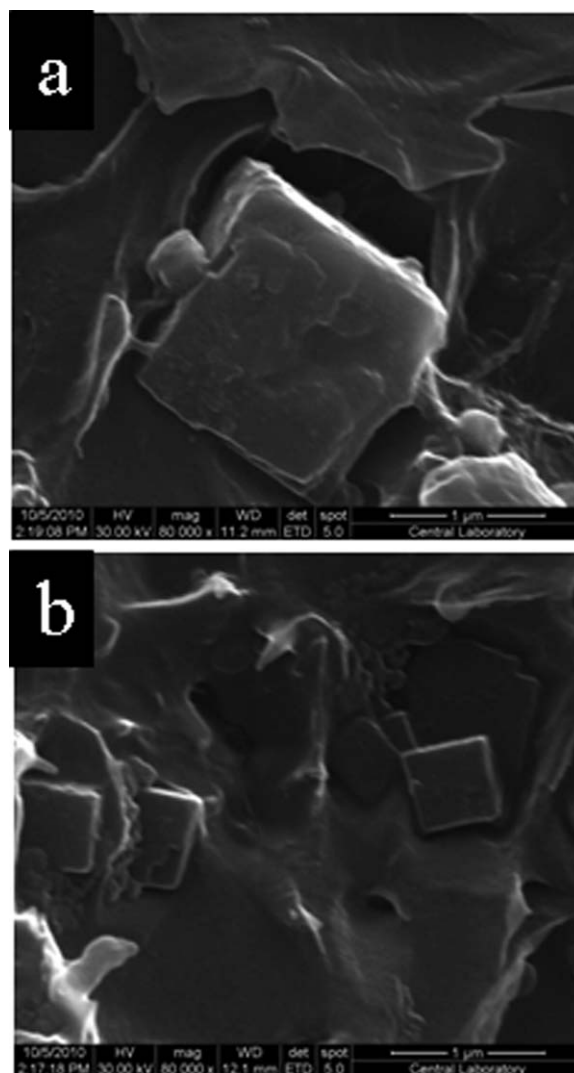


Figure 10. Cross-sectional SEM images of PES/SAPO-34 (a) and PES/HMA/SAPO-34 (b) membranes.

part of membrane structure permanently in the studied temperature range. Moreover, Topuz et al.²⁶ showed that HMA reduces the CO₂ and CH₄ sorption capacities of PES/SAPO-34 particles, which also causes lower permeabilities through membranes with HMA.

PES/SAPO-34-p and PES/HMA/SAPO-34-p membranes exhibited higher gas permeabilities than homogeneous PES-n and PES/HMA-p membranes. Permeation through zeolites is known to be an activated process, and diffusion through zeolites increase with temperature. On the other hand, incompatibility between zeolites and polymers shape voids around the zeolite particles in the MMMs, which has a pronounced effect on the gas permeation performance of those types of membranes.^{27,28} Therefore, high permeabilities through SAPO-34-containing membranes can be attributed to the microporous structure of SAPO-34 and voids formed around the SAPO-34 particles as it can be deduced from the SEM image of post-annealed PES/SAPO-34 membrane [Figure 10(a)].

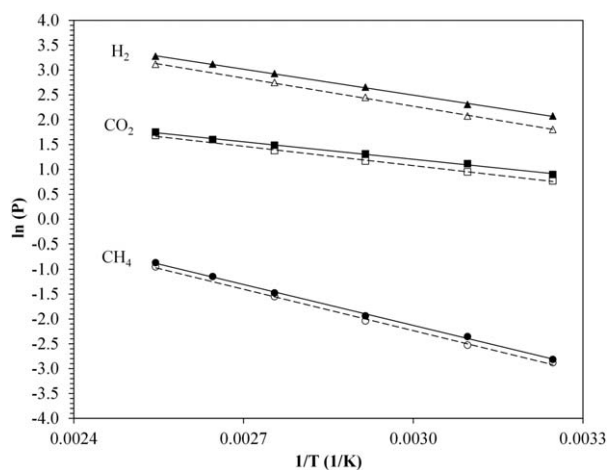


Figure 11. Influence of operating temperature on H_2 , CO_2 , and CH_4 permeabilities for post-annealed PES/HMA and PES/HMA/SAPO-34 membranes.

The natural logarithm of permeabilities decreased linearly with the reciprocal temperature for all membranes. This behavior, which is shown in Figure 11 for homogeneous PES/HMA-p and heterogeneous PES/SAPO-34/HMA-p membranes as an example, was correlated with the Arrhenius equation. Although Arrhenius equation is applicable typically for homogeneous polymeric membranes, it also fits well for heterogeneous membrane as shown.

Table I presents the activation energies of permeation for H_2 , CO_2 , and CH_4 . The activation energies were in the order of $CH_4 > H_2 > CO_2$ for all membranes. The activation energies for pure PES membrane are consistent with those in the literature.²⁵

Activation energy of permeation is a combination of activation energy of diffusion and the heat of sorption. Activation energy of diffusion increases with increasing size of the permeating molecule.^{3,29} CH_4 , which had the largest kinetic diameter among the studied gases, showed the highest resistance to make diffusive jumps. Hence, CH_4 had higher activation energy of permeation than that of H_2 and CO_2 . On the other hand, CO_2 was the most soluble gas and was of the lowest activation energy of permeation.

HMA acted as the antiplasticizing agent, which induced a stiffer backbone and yielded larger resistance for diffusion. Therefore, the activation energy to permeate was higher for HMA incorpo-

Table I. Activation Energies of Permeation through PES and Mixed Matrix Membranes

Membrane	Ea (kJ/mol)		
	H_2	CO_2	CH_4
PES	14.1	9.30	22.7
PES/HMA	15.7	10.7	24.3
PES/SAPO-34	13.4	8.42	21.3
PES/SAPO-34/HMA	14.5	9.62	22.8

rated membranes than for HMA-free membranes. Introducing SAPO-34 strongly influenced both diffusion and sorption characteristics of membranes, besides weak interaction between PES and SAPO-34 enabled the penetrant molecules to permeate more easily through the interfacial voids. As a result, the activation energies for PES/SAPO-34 membrane were lower than those of PES membrane. A similar relation was observed between PES/HMA/SAPO-34 and PES/HMA membranes. Addition of HMA to PES/SAPO-34 MMM increased the activation energies, and the activation energies came close to those of pure polymeric membrane, suggesting that HMA acts as a compatibilizer between the two phases.

Ideal selectivities were ranked in the following order: PES/HMA/SAPO-34 > PES/HMA > PES \approx PES/SAPO-34 (Tables I and II). Although the permeabilities were enhanced with increasing temperature, the H_2/CH_4 and CO_2/CH_4 ideal selectivities declined for all membranes. H_2/CH_4 selectivity of PES/HMA/SAPO-34 membrane was nearly 133 at 35°C, and it dropped to nearly 64 at 120°C. CO_2/CH_4 selectivity of the same membrane was 41.6 at low temperature and 13.7 at 120°C. In contrast, H_2/CO_2 selectivity exhibited a slight increase with temperature.

Selectivity of a membrane for a gas pair is a combination of diffusion and sorption selectivities. Diffusion coefficients of gases increase but diffusion selectivity may decrease with increasing temperature because of extended segmental motion of polymer chains at elevated temperatures. Solubility, which mainly depends on the polymer-penetrant interactions and chemical nature of the penetrating molecules, is also sensitive to temperature. Temperature influences the sorption selectivity to a larger extent if the difference in the condensability between the molecules increases. The diffusion coefficients and solubilities of the studied gases are likely to be in the order of $H_2 > CO_2 > CH_4$

Table II. Ideal Selectivities (α) of Membranes Without HMA as a Function of Temperature

T (°C)	α for PES membrane			α for PES/SAPO-34 membrane		
	H_2/CO_2	H_2/CH_4	CO_2/CH_4	H_2/CO_2	H_2/CH_4	CO_2/CH_4
35	2.08	71.7	34.5	2.14	70.0	32.7
50	2.26	58.9	26.1	2.31	62.6	27.1
70	2.56	50.8	19.8	2.57	53.1	20.7
90	2.74	41.4	15.1	2.92	44.3	15.2
35	2.07	73.3	35.4	2.14	70.8	33.1

Table III. Ideal Selectivities (α) of Membranes with HMA as a Function of Temperature

T (°C)	α for PES/HMA membrane			α for PES/SAPO-34/HMA membrane		
	H ₂ /CO ₂	H ₂ /CH ₄	CO ₂ /CH ₄	H ₂ /CO ₂	H ₂ /CH ₄	CO ₂ /CH ₄
35	2.81	110.4	39.3	3.20	132.8	41.6
50	3.07	103.4	33.6	3.29	105.5	32.1
70	3.60	89.2	24.8	3.80	98.6	25.8
90	3.94	71.1	18.1	4.23	81.7	19.3
105				4.56	71.0	15.6
120				4.60	63.5	13.7
35	2.78	107.2	38.6	3.23	126.7	39.2

and CO₂ > CH₄ > H₂, respectively. Therefore H₂/CH₄ and CO₂/CH₄ ideal selectivities decreased nearly 40% and 55% for all membranes by increasing the temperature from 35°C to 90°C, respectively. However, H₂/CO₂ selectivity increased by 35% (in average) in the same temperature range.

Although incorporation of SAPO-34 to PES improved the permeabilities, no effect of SAPO-34 was observed on the ideal selectivity (Table II). This suggests that the interfacial voids are the major reason of high permeabilities through PES/SAPO-34 membrane. However, introducing HMA resulted in a substantial improvement in ideal selectivities, which was especially pronounced for H₂/CH₄ ideal selectivity (Table III). The restricted segmental motion of polymer chains due to antiplasticization effect of HMA mainly influences the permeation of CH₄ molecule. It should also be noticed that PES/HMA/SAPO-34 membrane has higher ideal selectivities at all temperatures than PES/HMA, suggesting that HMA increases the compatibility between PES and SAPO-34 that can be seen in the SEM image of post-annealed PES/HMA/SAPO-34 membrane [Figure 10(b)].

After measurements at different temperatures for about 2 months, each membrane was tested at 35°C again. Almost the same permeabilities and ideal selectivities as the initial test were observed after final measurement at 35°C. These results clearly indicate the stability of all membranes. PES/SAPO-34/HMA ternary component membrane exhibited the best gas permeation performance at all temperature.

CONCLUSIONS

Annealing time and temperature affected the reproducibility and stability of the MMMs. By applying post-annealing step to MMMs at higher temperatures and longer times, membranes with more stable gas permeation performances were obtained.

The permeabilities of all studied gases increased with increasing operation temperature. The best separation performance belonged to PES/SAPO-34/HMA MMM at each temperature. The activation energies were found to be in the order of CH₄ > H₂ > CO₂ for all types of membranes. PES/SAPO-34/HMA membrane had activation energies higher than that of PES/SAPO-34 membrane and closer to that of pure PES membrane, which showed that HMA acts as a compatibilizer between the two phases.

ACKNOWLEDGMENTS

The authors thank METU Research Fund for financial support and METU Central Laboratories for analysis of membranes.

REFERENCES

- Robeson, L. M. *J. Membr. Sci.* **2008**, *320*, 390.
- Robeson, L. M.; Freeman, B. D.; Paul, D. R.; Rowe, B. W. *J. Membr. Sci.* **2009**, *341*, 178.
- Rowe, B. W.; Robeson, L. M.; Freeman, B. D.; Paul, D. R. *J. Membr. Sci.* **2010**, *360*, 58.
- Costello, L. M.; Koros, W. J. *J. Polym. Sci. Part B: Polym. Phys.* **1994**, *32*, 701.
- Lin, H.; Freeman, B. D. *J. Membr. Sci.* **2004**, *239*, 105.
- Chung, T. S.; Lin, W. H. *J. Membr. Sci.* **2001**, *186*, 183.
- Jha, P.; Way, J. D. *J. Membr. Sci.* **2008**, *324*, 151.
- Choi, S.; Coronas, J.; Lai, Z.; Yust, D.; Onorato, F.; Tsapatsis, M. *J. Membr. Sci.* **2008**, *316*, 145.
- Sen, D.; Kalipcilar, H.; Yilmaz, L. *J. Membr. Sci.* **2007**, *303*, 194.
- Li, Y.; Guan, H. M.; Chung, T. S.; Kulprathipanja, S. *J. Membr. Sci.* **2006**, *275*, 17.
- Yong, H. H.; Park, H. C.; Kang, Y. S.; Won, J.; Kim, W. N. *J. Membr. Sci.* **2010**, *188*, 151.
- Khan, A. L.; Cano-Odena, A.; Gutierrez, B.; Minguillon, C.; Vankelecom, F. J. *J. Membr. Sci.* **2010**, *350*, 340.
- Karatay, E.; Kalipcilar, H.; Yilmaz, L. *J. Membr. Sci.* **2010**, *364*, 75.
- Ulgen, C.; Kalipcilar, H.; Yilmaz, L. *J. Membr. Sci.* **2012**, *417–418*, 45.
- Hacarlioglu, P.; Toppare, L.; Yilmaz, L. *J. Appl. Polym. Sci.* **2002**, *90*, 776.
- Shen, Y.; Lua, A. C. *J. Appl. Polym. Sci.* **2010**, *116*, 2906.
- Maeda, Y.; Paul, D. R. *J. Membr. Sci.* **1987**, *30*, 1.
- Maeda, Y.; Paul, D. R. *J. Polym. Sci. Part B: Polym. Phys.* **1987**, *25*, 1005.
- Fu, Y. J.; Hu, C. C.; Qui, H.; Lee, K. R.; Lai, J. Y. *Sep. Purif. Technol.* **2008**, *63*, 175.

20. Joly, C.; Le Cerf, D.; Chappey, C.; Langevin, D.; Muller, G. *Sep. Purif. Technol.* **1999**, *16*, 47.
21. Ismail, A. F.; Rahim, R. A.; Rahman, W. A. W. A. *Sep. Purif. Technol.* **2008**, *63*, 200.
22. Wang, J.; Zheng, X.; Wu, H.; Zheng, B.; Jiang, Z.; Hao, X.; Wang, B. *J. Power Sources* **2008**, *178*, 9.
23. Smitha, B.; Sridhar, S.; Khan, A. A. *Eur. Polym. J.* **2005**, *41*, 1859.
24. Joly, B.; Le Cerf, D.; Chappey, C.; Langevin, D.; Muller, G. *Sep. Purif. Technol.* **1999**, *16*, 47.
25. Wang, D.; Li, K.; Teo, W. K. *J. Appl. Polym. Sci.* **1997**, *66*, 837.
26. Topuz, B.; Kalıpcılar, H.; Yılmaz, L. *J. Membr. Sci.* **2012**, *415*, 725.
27. Mahajan, R.; Koros, W. *J. Ind. Eng. Chem. Res.* **2000**, *39*, 2692.
28. Mahajan, R.; Koros, W. *J. Polym. Eng. Sci.* **2002**, *42*, 1420.
29. Alentiev, A. Y.; Yampolskii, Y. P. *J. Membr. Sci.* **2002**, *206*, 291.